

# DIRECT OPTIMIZATION METHOD AND AERODYNAMIC SHAPE DESIGN AT SUPERSONIC FLIGHT CONDITIONS

S.A. Takovitskii

Central Aerohydrodynamic Institute (TsAGI)

*Keywords: optimization, aerodynamic shapes, supersonic aircraft*

## Abstract

*The efficient method for aerodynamic shape profiling in supersonic flow is presented. The method combines Newton based optimization algorithm and flow modeling within the framework of Euler's equations system. The various design problems are considered: two-dimensional airfoils and axisymmetrical fore-bodies realizing minimum of a wave drag, the supersonic part of an axisymmetrical nozzle with maximum thrust, the simplest shape deformation of a complex plane form wing that ensures reduction of drag due to lift, profiling of fuselage and wing of a supersonic aircraft with high lift to drag ratio and low sonic boom. The objective functions are minimized under geometric and aerodynamic constraints.*

## 1 General Introduction

The present state of the art of computing and methods of mathematical modeling makes it possible to solve different problems concerning the choice of rational aerodynamic shapes. In [1-3] the classic research problems in supersonic flight were considered. Two-dimensional profiles, axisymmetric fuselages and fore-bodies that have minimum pressure drag in supersonic flow subject to a set of geometric constraints were constructed. The results were obtained within the framework of the Euler model over a wide range of the relevant parameters, namely, the Mach number and the enclosed area/volume or the aspect ratio. The aerodynamic shape optimization problems are ill-conditioned one and the simplest versatile methods (such as cyclic coordinate wise descent or gradient descent)

cannot ensure reliable solution. Even when relatively few parameters are varied, linear convergence (at the rate of a geometric progression) proves to be insufficient. The efficiency of direct optimization methods may be improved significantly by a proper choice of the system of geometrical parameters. Convergence acceleration is reached due to simplification of the variational problem statement [4]. A local analysis of the aerodynamic load distribution is used to study the aerodynamic functions behaviour allowing analytic formulation of the objective function and constraints. On the base of approximations to the true Hessian matrix and gradient vector the shape variations that enable the aerodynamic performance to be improved are established.

Another line of optimization research is related with the foundation of analytical solutions for the problem and studying characteristic features of optimal configurations. In the Newton model, the generatrices of the optimal fore-bodies of all possible aspect ratios are elements of a unique generatrix. The limit solution is the generatrix described by a power-law dependence of the fore-body radius on the longitudinal coordinate,  $r \sim x^n$ , with the exponent equal to  $\frac{3}{4}$  [5]. Numerical parametric studies of the fore-bodies with power-law generatrix showed that the theoretical value of the exponent was overestimated. The extremal value increases with the Mach number but does not exceed  $n=0.71$  [6]. A new reliable tool for solving optimization problems analytically is the method of small variations of the shape of bodies with a known distribution of the aerodynamic forces [7]. Assuming a local linear relationship between the pressure variation over a surface element and the increment of the

geometric parameters, the objective function can be approximated by a quadratic form. The conditions for the minimum of the objective function lead to the system of linear equations for determining the optimum geometric parameters. The method turned out to be effective for studying various design problems.

## 2 Two-dimensional airfoils with minimum wave drag

In local flow models the pressure at any point of the surface is related with the angle between the tangent to the body and the free-stream velocity. Thus, the variation of the gasdynamic functions with respect to the undisturbed conditions is evaluated. In order to increase the accuracy one can take the data obtained in the nonlinear formulation as the initial conditions. For example, the exact value of the pressure on a wedge can be determined in oblique shock theory. Prandtl-Meyer theory gives the pressure behind the break of the rhombus contour. These airfoils are used as the initial geometric shapes.

The airfoil contour with a pointed vertex is represented by a set of  $N+1$  segments (only the upper half of the airfoil is considered). The segments connect a sequence of points with coordinates  $x_0=0$  and  $y_0=0$ ,  $x_1$  and  $y_1$ , ...,  $x_{N-1}$  and  $y_{N-1}$ ,  $x_N=1$  and  $y_N$ ,  $x_{N+1}=1$  and  $y_{N+1}=0$ . The airfoil length is equal to  $x_N - x_0=1$ . The distribution of the segments is assumed to be uniform:  $x_n=n/N$ ,  $n=1...N$ . The last segment represents the base section and has zero length when the trailing edge is sharp. The wave drag coefficient can be represented by the sum

$$C_D = \frac{2}{0.5\rho_\infty V_\infty^2} \sum_{n=1}^{N+1} p_n (y_n - y_{n-1})$$

where  $p_n$  is the pressure for the  $n$ th segment and  $0.5\rho_\infty V_\infty^2$  is free-stream dynamic pressure.

It is assumed that the airfoil is slender and the base pressure  $p_{N+1}=p_b$  is known and does not vary with variation of the airfoil shape. For weak waves and small deformations the relation between the pressure and the geometric parameters is given by the expression

$$\Delta p_n = \frac{\gamma M_n^2 p_n (\Delta y_n - \Delta y_{n-1})}{\sqrt{M_n^2 - 1} (x_n - x_{n-1})} = r_n (\Delta y_n - \Delta y_{n-1})$$

where  $M_n$  is the Mach number for the  $n$ th segment,  $\Delta p_n$ ,  $\Delta y_n$  and  $\Delta y_{n-1}$  are the changes in the pressure and the ordinates of the endpoints of the  $n$ th segment, and  $\gamma$  is the specific heat ratio.

Summation of the loading over the airfoil contour gives an approximation of the objective function (wave drag variation) as quadratic form

$$\Delta C_D = \frac{2}{0.5\rho_\infty V_\infty^2} \left\{ \sum_{n=1}^N [(p_n + r_n (y_n - y_{n-1})) (\Delta y_n - \Delta y_{n-1}) + r_n (\Delta y_n - \Delta y_{n-1})^2] - p_b \Delta y_N \right\}$$

The problem becomes redundant without suitable constraint. The airfoil is constructed under condition of conservation of enclosed area  $S$ . Introducing the Lagrangian function  $F = \Delta C_D + \lambda \Delta S$  with a multiplier  $\lambda$  and differentiating it with respect to the independent variables, we obtain the following system of  $N+1$  linear equations for determining the optimum variation of the shape

$$2\Delta y_1 + 2\Delta y_2 + \dots + 2\Delta y_{N-1} + \Delta y_N = 0$$

$$2\lambda + p_1 + r_1 y_1 - p_2 - r_2 (y_2 - y_1) + 2(r_1 + r_2) \Delta y_1 - 2r_2 \Delta y_2 = 0$$

$$2\lambda + p_2 + r_2 (y_2 - y_1) - p_3 - r_3 (y_3 - y_2) + 2(r_2 + r_3) \Delta y_2 - 2r_2 \Delta y_1 - 2r_3 \Delta y_3 = 0$$

...

$$2\lambda + p_{N-1} + r_{N-1} (y_{N-1} - y_{N-2}) - p_N - r_N (y_N - y_{N-1}) + 2(r_{N-1} + r_N) \Delta y_{N-1} - 2r_{N-1} \Delta y_{N-2} - 2r_N \Delta y_N = 0$$

$$\lambda + p_N + r_N (y_N - y_{N-1}) - p_b + 2r_N \Delta y_N - 2r_N \Delta y_{N-1} = 0$$

After simple algebra we obtain the representations for the Lagrangian multiplier and the ordinate variations in terms of the first point ordinate variation  $\Delta y_1$ .

$$\lambda = -[p_1 - p_b + r_1 (y_1 + 2\Delta y_1)] / (2N - 1)$$

$$\Delta y_n = \frac{1}{2N - 1} \sum_{i=1}^n [(2N - i)(p_1 + r_1 (y_1 + \Delta y_1)) +$$

$$+ (i - 1)(p_b - r_1 \Delta y_1) - (2N - 1)(p_i + r_i (y_i - y_{i-1}))] r_i^{-1}$$

Extremum value of  $\Delta y_1$  is determined from the condition of enclosed area conservation.

In order to find the analytic solution of the problem and construct the airfoils with and without end face, the wedge with the half angle  $\delta_w = \arctg(S)$  and the rhombus with the half angle  $\delta_r = \arctg(2S)$  are taken as the initial airfoils.

At first case the following relations hold:  $y_n = x_n \tg \delta$ ,  $p_n = p_s$ ,  $M_n = M_s$ , where  $p_s$  and  $M_s$  are the pressure and the Mach number behind the

oblique shock. The extremum variation of the  $n$ th ordinate is expressed as

$$\Delta y_n = \left[ tg\delta + \frac{\sqrt{M_s^2 - 1}}{\gamma M_s^2} \left( 1 - \frac{p_b}{p_s} \right) \right] \frac{n(2N^2 - 3nN + 1)}{2N(4N^2 - 1)}$$

On passing to the limit as  $N \rightarrow \infty$ , we go over to the continuous dependence

$$\Delta y = \frac{1}{8} \left[ tg\delta + \frac{\sqrt{M_s^2 - 1}}{\gamma M_s^2} \left( 1 - \frac{p_b}{p_s} \right) \right] (2 - 3x)x$$

Thus, the optimum variation of the wedge contour is a parabola with vertex at  $x=1/3$  which intersects the  $X$  axis at the points  $x=0$  and  $x=2/3$ .

At the second case for the first  $N/2$  segments of the rhombus the pressure  $p_s$  and the Mach number  $M_s$  correspond to the conditions behind the oblique shock. For the remaining  $N/2$  segments located behind the contour break the pressure  $p_v$  and the Mach number  $M_v$  are determined from the Prandtl-Meyer theory. The pressure variation on the  $n$ th segment is

$$\Delta p_n = r_i (\Delta y_n - \Delta y_{n-1})$$

$$r_i = \gamma M_i^2 p_i N / \sqrt{M_i^2 - 1}$$

$$i = \begin{cases} s, & n \leq N/2 \\ v, & n > N/2 \end{cases}$$

The contour of the optimum airfoil with sharp edges is formed by two parabolic segments

$$y = 1.5S\bar{x} \left( 3 + (r_s r_v)^q - 4\bar{x} \right) \left( 1 + (r_s r_v)^q \right)^{-1}$$

$$\bar{x} = x \text{ and } q = 1 \text{ if } x \leq 0.5;$$

$$\bar{x} = 1 - x \text{ and } q = -1 \text{ if } x > 0.5$$

Setting  $r_s = r_v$  gives the well-known parabolic airfoil symmetric about the middle of the chord. This solution is the limiting one as  $S \rightarrow 0$ . For nonzero values of enclosed area the thickness of the optimum airfoil is greater than thickness of the airfoil obtained, assuming a linearized flow model. The enclosed area is redistributed farther from the vertex. The rhombus, parabolic and optimal airfoils at Mach number  $M=3$  and  $S=0.192$  are compared in fig.1.

The optimal airfoils are slightly different for different Mach numbers. The nonlinear optimization reduces the magnitude of the leading edge shock. As compared with the parabolic airfoils, the optimal airfoils give a

gain in the wave drag greater than 30% at  $M=12$  (fig. 2).

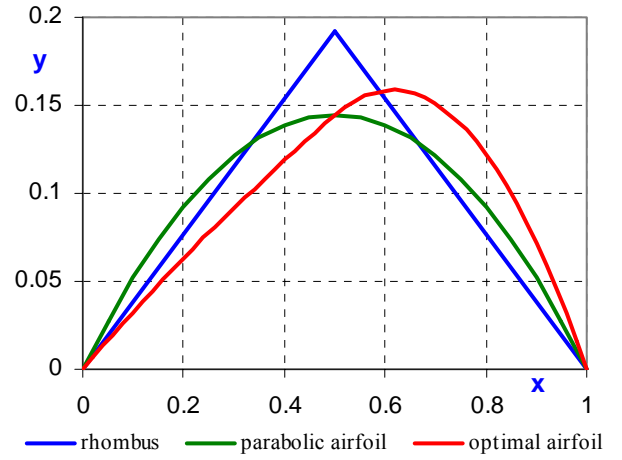


Fig. 1. Airfoils ( $M=3$ ,  $S=0.192$ )

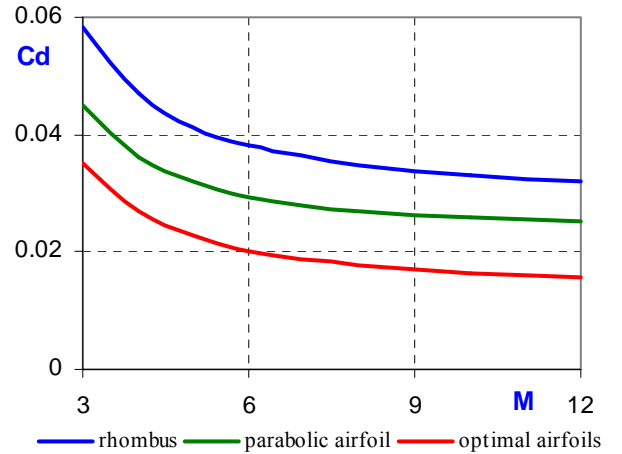


Fig. 2. Wave drag coefficient ( $S=0.192$ )

### 3 Axisymmetric fore-bodies with minimum wave drag

In the case of axisymmetric fore-bodies with a given aspect ratio, the flow fields behind the attached shocks on cones are known and the solution is constructed as an improving variation to the conical shape. It is shown that the near-optimal fore-bodies have a flat forward face and a power-law generatrix with the exponent equal to  $2/3$ . The only parameter dependent on the free stream Mach number and the fore-body aspect ratio  $\lambda=L/2R$  ( $L$  – the fore-body length,  $R$  – the base radius) is the forward face radius  $r_1$ . For the fore-body generatrix the following dependence of the radius on the longitudinal coordinate is proposed

$$r = \frac{L}{2\lambda} \left[ \left( \frac{2\lambda r_1}{L} \right)^{3/2} + \left( 1 - \left( \frac{2\lambda r_1}{L} \right)^{3/2} \right) \frac{x}{L} \right]^{2/3}$$

By varying  $r_1$  one can solve the extremum problem for the function of the single variable and thus find the truncated power-law fore-body of minimum wave drag. The ratio of the forward face radius to that of the base decreases with increase of the aspect ratio and Mach number.

The limiting solution for  $\lambda \rightarrow \infty$  is the power-law fore-body  $r/R=(x/L)^{2/3}$ . The exponent  $2/3$  differs from well known result of Newton's model  $-3/4$ . The aerodynamic drag of Newton's theory fore-body increases on longitudinal coordinate as a linear function, in the framework of the accepted simplified model the derivative  $dC_D/dx=const$ . This result is not correct for the optimum fore-bodies. The aerodynamic drag increases in much the same way to a linear function of the radial coordinate  $-dC_D/dr \approx const$ . Common characteristic feature of the optimum fore-bodies is demonstrated in fig. 3.

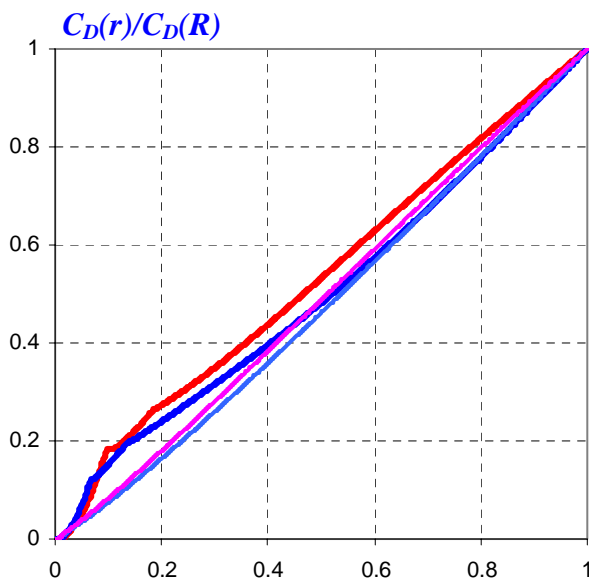


Fig. 3. Wave drag rise on radial coordinate

- optimum fore-body (M=2, λ=2)
- optimum fore-body (M=4, λ=2)
- power-law fore-body (M=2, λ=16)
- power-law fore-body (M=4, λ=16)

The wave drags of various fore-bodies are compared in fig. 4. The first near to optimum shapes, found by Newton, are characterized by the presence of a front face. A solution of the problem within the framework of slender body

theory was obtained by Karman. When the aspect ratio is increased the optimum size of the front face rapidly decreases. As result the front face contribution to the total wave drag is reduced and near to optimum pointed nose shapes could be constructed [3]. The proposed truncated power-law fore-bodies are slightly different from the optimal fore-bodies [1] that give a gain in drag not greater than 3% at M=2 and not greater than 1% at M=4. The greatest discrepancy is observed at small ( $\lambda=1$ ) and large ( $\lambda=8$ ) aspect ratios.

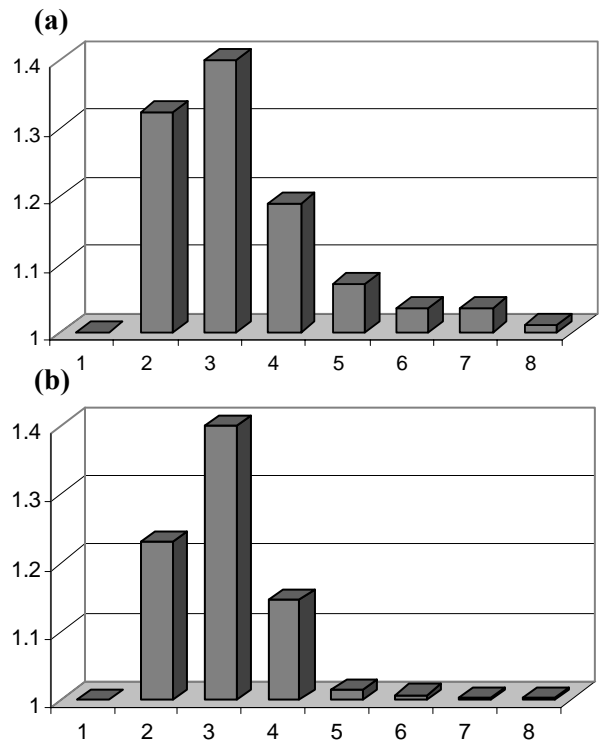


Fig. 4. Comparison of drag coefficient  $C_D/C_{D_{min}}$  at M=2, λ=2 (a); M=4, λ=4 (b)

- 1 – optimum fore-body [1]; 2 – cone; 3 – parabolic fore-body; 4 – von Karman ogive; 5 – Newton's theory fore-body; 6 – power-law fore-body [6]; 7 – pointed optimum fore-body [3]; 8 – truncated power-law fore-body

It should be noted that optimal fore-body shapes differ significantly from the shapes defined on the base of Newton pressure equation (fig. 5). On values of the wave drag relative difference exceeds 25% for noses of small aspect ratio. The radius of the front face of Newton fore-body is twice smaller. With increase of Mach number the reliability of Newton theory grows. But geometrical parameters are still different significantly.

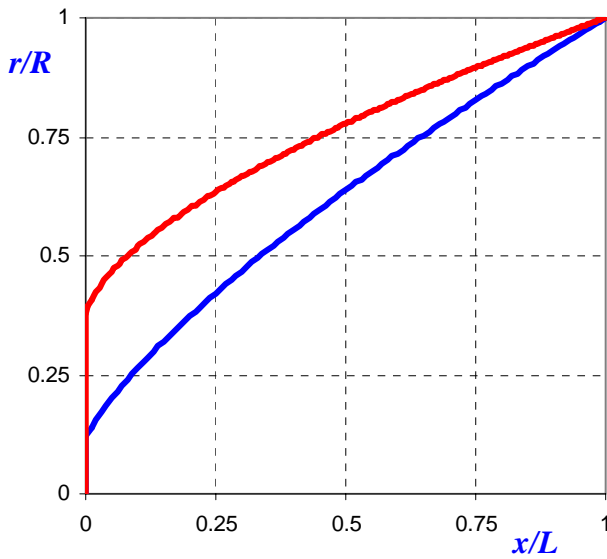


Fig. 5. Generatrices of the optimum forebodies ( $M=1.5$ ,  $\lambda=1$ )

— Euler flow model    — Newton flow model

#### 4 Supersonic nozzles with maximum exhaust thrust

The nozzle shape is profiled to realize maximum exhaust thrust under given restrictions on the overall dimensions. As distinct from the problems of external aerodynamics, in this case simplified flow models based on local relations between the geometric and gasdynamic parameters have not found wide application. On the one hand, this is due to the restricted possibilities of local approaches. In particular, the Newton formula for the pressure is applicable only to windward surfaces. On the other hand, the modern state of computer technology makes it possible to solve optimization problems on the basis of the most accurate flow models [8].

At the same time, the study of the characteristic features of optimal configurations remains topical. On the base of the method of small variations of the geometrical parameters it is determined near to optimal nozzle generatrix represented by a power-law dependence of the radius on the longitudinal coordinate [9].

The solution is a power-law function of the form  $r=(A+Bx)^{2/3}$ . The coefficients  $A$  and  $B$  are determined from the boundary conditions. The first boundary condition is imposed in one of

the sections in the vicinity of the entry section of the nozzle or directly in that section, depending on the presence or absence of a constraint on the nozzle contour curvature. In the latter case we have  $r=1$  at  $x=0$  (the entry section radius is taken as the scale length) and, therefore,  $A=1$ . In the former case we find the section in which a smooth junction between the circle and the power-law generatrix is ensured. One of the form parameters remains free. It is required to compare the thrust characteristics of nozzles differing in exit section diameter (the only independent parameter) and to choose the optimal configuration.

Three optimal nozzles are found for next conditions: length  $L=20$  and curvature radius at the entry section  $R=0.5$ . The first nozzle has a linear generatrix and the second has a power-law generatrix. In both cases the optimum is determined by varying a single parameter, namely, the nozzle exit section diameter. The third nozzle was obtained using the direct optimization method.

The nozzle with a linear generatrix has the greatest area ratio; its exit section area is about 15% greater than that of the nozzle designed using numerical optimization. Despite this, the conical surface gives the least increase in exhaust thrust. The power-law nozzles are intermediate with respect to both the geometric and the force characteristics.

The optimal nozzles are compared in fig. 6. The internal flowfields are presented in the form of Mach number contours. The contours are plotted with a step  $\Delta M=0.5$ , the contour nearest to the initial section corresponding to the Mach number 1.5. The flows in the nozzles with curvilinear generatrix have a similar structure. In the central part of the flow an extended low-pressure region is located. In the conical nozzle the flow parameters are distributed more uniformly in the radial direction.

The power-law nozzles rank below the optimally designed nozzles by not more than 0.26% in thrust (or 1% in the aerodynamic force on the nozzle surface). Going over from conical nozzles to nozzles with curvilinear generatrices leads to a considerable (up to 1.4%) increase in the thrust. In this case, more than 75% of the

greatest possible thrust increase is achieved using power-law nozzles.

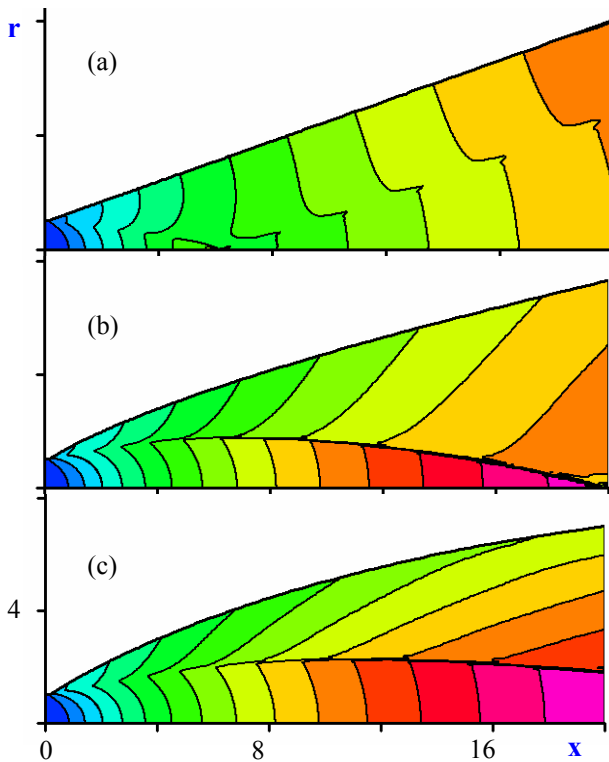


Fig. 6. Mach number contours ( $\Delta M=0.5$ ) in nozzles with linear (a), power-law (b), and numerically optimized (c) generatrix

## 5 Supersonic aircraft

The aircraft designed for cruise flight at Mach number  $M=1.8$ , altitude  $H=16$  kilometers is considered. Aircraft weight is  $W=50\,000$  kilograms. The fuselage length is  $L=40$  meters. Plane view wing area is  $S=160$  square meters. The fuselage interior volume is  $V=120$  cubic meters. Wing is performed with cranked leading-edge and trailing-edge (fig. 7).

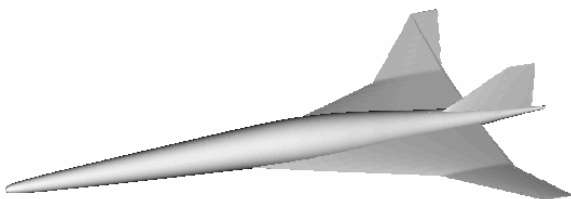


Fig. 7. Supersonic aircraft

Aerodynamic drag and sonic boom signature parameters are used as the objective functions minimized under geometric and aerodynamic constraints. Flow field near the aircraft is modeled within the framework of Euler equations. A gas-dynamic properties jump on a head shock wave is allocated strictly. Inside shock waves and other flow discontinuities are treated without tracking their spatial location. The computation mesh is constructed by the multi-zone approach. The surface friction drag is determined by a semiempirical calculation method for a turbulent boundary layer.

The opportunity of reduction of lift induced drag by means of the simplest deformations established earlier for delta wing [10] is investigated for complex plane form wing. The wing median surface is represented by four flat elements joined along lines passing through the wing top. Near to conic deformation of the wing provides up to 90% of total decrease of drag due to lift. It confirms importance of researches on definition of the simple deformations in problems of aerodynamic forms optimization.

Sonic boom pressure signatures for given cruise Mach number, altitude, and aircraft geometry parameters are computed according to geometric acoustic theory with nonlinear effects accounted. Sonic boom propagation in a horizontally stratified atmosphere is modeled. The case of steady flight and no winds is studied. Sonic boom waveforms are found directly below the aircraft flight path.

The problem is solved through two stages. At the first stage, F-function is determined. Lift contribution to sonic boom is taken into account on the base of supersonic area rule theory. Equivalent area derivatives are related with disturbances of velocity [11]. Asymptotic dependence of pressure on time (or on longitudinal coordinate) and corresponding F-function are obtained on the base of flow parameters in a narrow vicinity of the aircraft. At the second stage, pressure signatures far away from the aircraft at a desired distance from the ground or on the ground are determined using reliable acoustic methods [12, 13].

Optimization is performed without restriction on rear shock. Fore part of pressure

signature with initial shock is analyzed. The initial shock intensity as the primary value of the pressure signature is minimized. Overpressure levels are allowed to rise following the initial shock. The rate of rise in this signature is controlled and equals the rate of decrease after maximal overpressure in absolute value. Sonic boom minimizing equivalent area distribution is determined by three parameter power law [14].

During optimization the fuselage of round cross section is modified by means of internal volume redistribution in longitudinal direction and by cambering of fuselage axis. Starting fuselage is constructed in accordance with Sears-Haack body.

The wing is assumed to have the constant shape in the plane view. The flat wing with symmetrical profiles is taken as a starting one. The relative thickness of the wing profiles is 3%. It is allowed to redistribute interior volume in longitudinal direction only. For the wing 21 longitudinal sections are allocated, each of which is partitioned into 20 segments. The nodal points define the apexes of triangular elements forming the upper and lower wing surfaces. Geometrical parameters are stated as displacements of nodal points in the normal direction to the base plane.

Theoretical analysis shows opportunity of significant mitigation of sonic boom. The initial shock intensity is 67 Pa for the starting aircraft

and 25 Pa for optimum equivalent body of revolution. Ground reflection factor equals 2.

The optimal wing forms are found for different problem statements. At the first statement aerodynamic drag is used as the objective function (wing 1). At the second statement the objective function is defined as displacement between F-function (or derivatives of equivalent cross section area) distributions for the aircraft and the optimal equivalent body of revolution (wing 2). At all cases the aircraft has equal fuselage corresponding to the second problem statement.

Geometric parameters of the fuselage are shown in fig. 8. Dependences of fuselage radius  $R$  on longitudinal coordinate reveal thickening of the fuselage nose. Fore-half of the fuselage is inclined downwards.

Geometric parameters of the wings are rather different. Wing 1 is characterized by negative values of twist angle. In absolute value twist angle increases from root chord to tip chord. Twist angle of wing 2 is positive and decreases along span of inboard part. After leading edge kink twist angle increases. Near the tip edge sections have maximal twist. Median lines of the wings are represented in fig.9 for three longitudinal sections. Span of the half wing is adopted as reference value. Root section of wing 2 has windward camber. The console part of the wing is convex in the lee side. Displacement of the trailing edge provides positive dihedral angle.

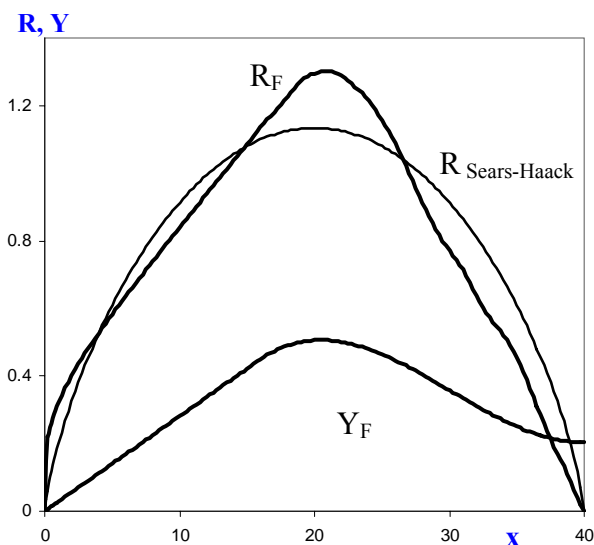


Fig. 8. Fuselage radius  $R$  and centerline  $Y$

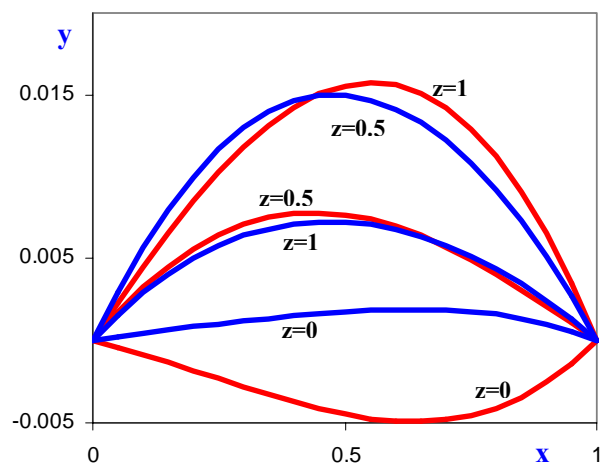


Fig. 9. Median lines

— wing 1 — wing 2

Results of sonic boom modeling for the aircrafts with optimal wings and for the optimal equivalent body of revolution are represented in fig. 10. Deformation of the wing (problem statement 2) aligns distributions of F-function. As result pressure disturbance signature on the ground consists of a number of successive weak shocks. Intensity of initial shock is 28 Pa. In case of wing 1 pressure jump increase up to 53 Pa. At the same time, the wing optimization at the problem statement 1 allows increasing of aircraft lift-to-drag ratio  $L/D$  at 12%.

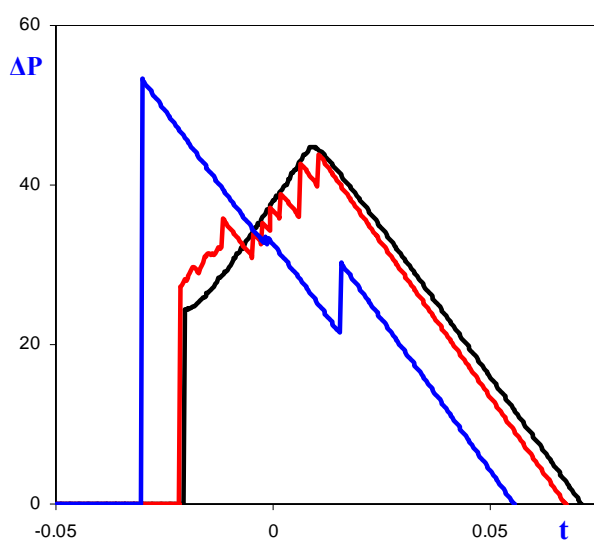


Fig. 10. Pressure signature  
 — wing 1 — wing 2  
 — equivalent body of revolution

## Acknowledgments

This work was supported by the Russian Foundation for Basic Research, project No. 10-01-00208a.

## References

- [1] Kraiko A.N., Pudovikov D.E., P'yankov K.S., and Tillyaeva N.I. Axisymmetric noses with a given aspect ratio optimal and near-optimal for wave drag. *Prikl. Mat. Mekh.*, Vol. 67, No. 5, 2003.
- [2] Palaniappan K. and Jameson A. Bodies having minimum pressure drag in supersonic flow – investigating nonlinear effects. *Proc. 22<sup>nd</sup> Applied Aerodynamics Conference and Exhibit*, Providence, Rhode Island, AIAA Paper 2004-5383, 2004.
- [3] Takovitskii S.A. Pointed two-parameter power-law nose shapes of minimum wave drag. *Prikl. Mat. Mekh.*, Vol. 67, No. 5, 2003.

- [4] Takovitsky S.A. Numerical optimization of the wing of a supersonic airplane. *Proc. 23<sup>rd</sup> Intern. Congr. of Aeronaut. Sci. (ICAS)*. Toronto, Canada, P. 232.1–232.7, 2002.
- [5] Eggers A.J. Jr., Resnikoff M.M., and Dennis D.H. Bodies of revolution having minimum drag at high supersonic air speeds. *NACA Report*, No. 1307, 1957.
- [6] Grodzovskii G.L. (ed.). *Aeromechanics of the supersonic flow past power-law bodies of revolution*. Mashinostroenie, Moscow, 1975, [in Russian].
- [7] Takovitskii S.A. Analytic solution in the problem of constructing an airfoil with minimum wave drag. *Fluid Dynamic*, Vol. 38, No. 6, 2003.
- [8] Kraiko A.N., Myshenkov E.V., P'yankov K.S., and Tillyaeva N.I. Effect of gas non-ideality on the performance of laval nozzles with an abrupt constriction. *Fluid Dynamics*, Vol. 37, No. 5, 2002.
- [9] Takovitskii S.A. Optimal supersonic nozzles with power-law generators. *Fluid Dynamics*, Vol. 44, No. 1, 2009.
- [10] Takovitskii S.A. The choice of the system of geometric parameters of an optimized wing. *J. Appl. Maths Mechs*, Vol. 62, No. 5, 1998.
- [11] Zilin Yu.L. and Kovalenko V.V. On matching the near-field and far-field profiles in the sonic boom problem. *Uchenye zapiski TsAGI*, Vol. 29, No. 3-4, 1998, [in Russian].
- [12] Hayes W.D., Haefeli R.C., and Kulsrud H.E. Sonic boom propagation in a stratified atmosphere, with computer program. *NASA CR-1299*, 1969.
- [13] George A.R. and Plotkin K.J. Sonic boom waveforms and amplitudes in a real atmosphere. *AIAA journal*, Vol. 7, No. 10, 1969.
- [14] Darden C.M. Minimization of sonic-boom parameters in real and isothermal atmospheres. *NASA TN D-7842*, 1975.

## Contact Author Email Address

[c.a.t@tsagi.ru](mailto:c.a.t@tsagi.ru)

## Copyright Statement

The authors confirm that they, and/or their company or organization, hold copyright on all of the original material included in this paper. The authors also confirm that they have obtained permission, from the copyright holder of any third party material included in this paper, to publish it as part of their paper. The authors confirm that they give permission, or have obtained permission from the copyright holder of this paper, for the publication and distribution of this paper as part of the ICAS2010 proceedings or as individual off-prints from the proceedings.